NANO LETTERS

LETTER

pubs.acs.org/NanoLett

Patchy Multishell Segregation in Pd−Pt Alloy Nanoparticles

Giovanni Barcaro,[†] Alessandro Fortunelli,*[,†] Micha Polak,[‡] and Leonid Rubinovich[‡]

[†]CNR-IPCF, Istituto per i Processi Chimico-Fisici, I-56124 Pisa, Italy

[‡] Department of Chemistry, Ben-Gurion University, Beer-Sheva 84105, Israel

Supporting Information

ABSTRACT: Chemical ordering in face-centered-cubic-like PdPt nanoparticles consisting of 38−201 atoms is studied via density-functional calculations combined with a symmetry orbit approach. It is found that for larger particles in the Pd-rich regime, Pt atoms can segregate at the center of the nanoparticle (111) surface facets, in contrast with extended systems in which Pd is known to segregate at the surface of alloy planar surfaces. In a range of compositions around 1:1, a novel multishell chemical ordering pattern was favored, in which each shell is a patchwork of islands of atoms of the two elements, but the order of the patchwork is reversed in the alternating shells. These findings are rationalized in terms of coordination-dependent bond-energy variations in the metal−metal interactions, and their implications in terms of properties and applications of nanoscale alloy particles are discussed.

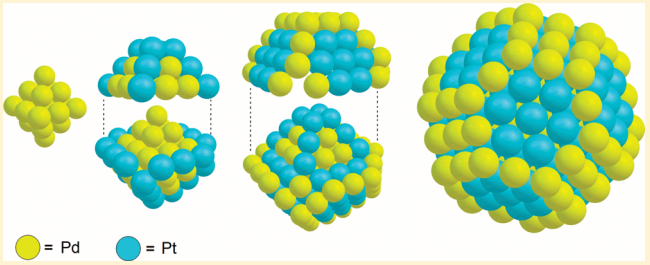

KEYWORDS: Nanoalloys, chemical ordering, surface segregation, metal nanoparticles, DFT calculations

In addition to structural morphology, the chemical ordering or compositional structure (i.e., the distribution of the different chemical species within a given structure)[1,2] plays a fundamental role in determining the properties of multicomponent metallic nanoparticles—or nanoalloys.[3,4] AgAu particles, for example, exhibit a different optical response depending on whether they are core−shell or random solutions.[5] Mechanical properties are equally known to be strongly affected by surface segregation.[6,7] The precise arrangement of the species in the particle is also important in catalysis, dominated by processes occurring at surface or subsurface shells, and changes in the segregation pattern under operating conditions have been observed.[8] Several mixing patterns have been described in the literature,[4] such as core−shell or in general multishell ordering (in which concentric shells of different elements alternate), random solutions, ordered arrangements (more or less related to the known ordered phases of bulk alloys), and Janus-like segregation typical of immiscible components.[9] In this context, theoretical methods can provide relevant information which nicely complements and sometimes prefigures experiment, but the prediction of the correct chemical ordering is not an easy task, especially at the first-principles level, due to the combinatorial increase in the number of possible "homotops" (isomers sharing the same skeletal structure and composition but differing in the mixing pattern).[3] Neglecting the reduction due to point group symmetry, for a cluster with given structure and N_{tot} atoms of which N_A of species A and N_B of species B, one has $(N_{tot})!/((N_A)!(N_B)!)$ possible different homotops. A possible solution to this problem is to consider "magic" structures,[10] i.e., arrangements exhibiting structural shell closure and thus exhibiting high symmetry. In this approach[10] the full point group symmetry is exploited to partition the atoms into "symmetry orbits",[11] i.e., groups of symmetry-equivalent species. The degrees of freedom of the system are thus reduced from N_{tot} to the number of symmetry-inequivalent orbits, N_{orb}, and correspondingly the number of distinct homotops is exponentially decreased.

In this work we adopt this symmetry orbit approach and apply it at a first-principles density-functional theory (DFT) level to study the segregation patterns of face-centered-cubic-like (fcc-like) PdPt nanoparticles in the size range between 38 and 201 atoms and over a broad range of compositions. We find that the interplay of metal−metal homo- and heterointeractions produces an unusual Pt surface segregation in Pd-rich particles (in spite of the larger Pt bulk energy) and a novel multishell pattern around equimolar composition in which each shell is decorated by "patches" of like atoms. We conclude by speculating on possible implications of these findings.

Plane-wave DFT calculations were performed using the QuantumEspresso package[12] employing ultrasoft pseudopotentials[13] and the Perdew−Burke−Ernzerhof (PBE) exchange-correlation (xc-) functional[14] (more details in the Supporting Information). Our structural models consist of fcc-like truncated octahedra (TO) configurations. Starting from octahedra, fcc polyhedra are obtained by truncating symmetrically their six vertices, obtaining square and hexagonal (or triangular) facets; see Figures 1 and 2. A given TO is characterized by two indexes: n_L, i.e., the length of the edge of the complete octahedron and n_{cut}, i.e., the number of layers cut at each vertex, and will be denoted as TO(n_L, n_{cut}) in the following. fcc-like structures are reasonable for PdPt particles at this size: the transition from icosahedral structures to less strained

Received: January 27, 2011
Published: March 02, 2011

structures is expected to occur at relatively small sizes for both Pd and Pt bare clusters,[15] and the only competitors to fcc motifs are decahedral or "hybrid" ones.[16] We select the site population within these models by applying the symmetry orbit approach in the O_h symmetry group. Broken-symmetry (such as Janus-like[9]) configurations have been explored but found very disfavored due to the strong mixing tendency of the Pd−Pt pair. The use of symmetry reduces the degrees of freedom of the system to N_{orb}, the number of symmetry-inequivalent orbits, which is 12 for a TO particle of 201 atoms. Considering that a full exploration of all possible symmetry-constrained segregation pattern is achieved by performing $2^{N_{orb}}$ calculations, it follows that this task is feasible using tight-binding Hamiltonians[10] or empirical potentials[11,16,17] but remains heavy to accomplish at the first-principles level due to limitations in computational resources. We have thus further reduced the number of possible homotops by focusing on selected compositions: the two regimes characterized by a small amount of one of the two elemental components and around 1:1 composition. An issue with the orbit approach is that the number of atoms in each orbit presents an nonhomogeneous distribution, being 1, 6, 12, or 24 in the cases here investigated. This puts constraints on the cluster chemical composition by limiting the number of homotops. To explore a broader range, a suborbit approach has been used, in which each orbit is divided into equivalent suborbits of six atoms. By properly choosing the populations of the suborbits in order to keep as high a symmetry as possible and to avoid repeated calculation of homologous configurations, it is possible to enlarge the scope of significant results still keeping the computational effort within reasonable limits. Four different sizes with N_{tot} = 38, 79, 116, 201 have been investigated, and total energy results for all selected homotops are reported in the Supporting Information.

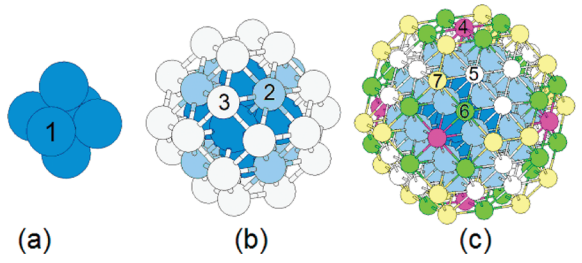

Figure 1. Orbit structure of the even-numbered truncated octahedra considered in this work: (a) 6-atom TO(2,0); (b) 38-atom TO(4,1), obtained adding 32 atoms to (a); (c) 116-atom TO(6,2), obtained adding 78 atoms to (b). Different symmetry orbits are singled out by different colors and numbers.

38-Atom Particle. This structure corresponds to the TO(4,1) shown in Figure 1b. It is made by an inner shell of 6 atoms (Figure 1a) and an outer shell of 32 atoms. The number of orbits is three: orbit-1 is formed by atoms of the inner shell; orbit-2 by the 8 atoms at the center of the (111) facets, and orbit-3 by the 24 atoms on the (100) facets.

A single Pd impurity in a nearly pure Pt cluster is best positioned on the surface, almost isoenergetically on the (111) or the (100) facets, while moving the Pd impurity into the core costs 0.23 eV. This is coherent with the lower surface energies of Pd, which thus prefers to segregate to the surface of the cluster.[18,19] At variance, a single Pt impurity can stay almost isoenergetically in the first or in the second orbit (i.e., in the core or on one of the 111 facets), whereas the occupation of the third orbit (one of the corners of the TO) increases the energy by 0.24 eV. This unexpected result (one could think that surface occupation by Pt is always disfavored with respect to the core) is the first indication of the Pt tendency to (111)-surface segregation. Increasing the number of impurity atoms to six changes the situation which turns out to be more in line with previous work,[20] as the six Pt atoms in fact preferentially go inside the cluster resulting in a core−shell structure.

79-Atom Particle. This structure corresponds to the TO(5,1) shown in Figure 2c. It is composed of three shells: the first shell is formed by the central atom (Figure 2a); the second shell by the surface of the internal (3,0) octahedron (Figure 2b); the third shell by the remaining 60 surface atoms. There are six orbits: orbit-1 corresponds to the central atom; orbit-2 to the surface of the inner TO(3,1) and contains 12 atoms; orbit-3 by the 6 vertices of the TO(3,0). The orbits from the fourth to the sixth contain the 60 surface atoms of the third shell: 24 on (111) facets (orbit 4), 12 on edges (orbit 5), and 24 on (100) facets (orbit 6).

For a single impurity the results are similar to those found in the 38 atoms case: a single Pt prefers to stay in the first inner-shell orbit, while moving it toward the surface corresponds to a gradual increase in the energy, with the situation mirrored in an inverse way for the Pd impurity. At the 6-73 composition, in Pt-rich structures the six Pd atoms prefer to populate corners, as expected, but for Pd-rich structures the landscape is more interesting. The lowest-energy configuration is one in which the Pt atoms populate part of the second orbit, which is not surprising as these sites are internal ones. However, this configuration is nearly isoenergetic with the occupation of the third and fourth orbit, which latter corresponds to a surface segregation of the Pt atoms in the middle of the external (111) facets. This behavior is definitively more marked at composition 12-67. Again, the Pt-rich panorama does not bear any surprise and the 12 Pd atoms preferentially populate the (100) facets. On the contrary, in the

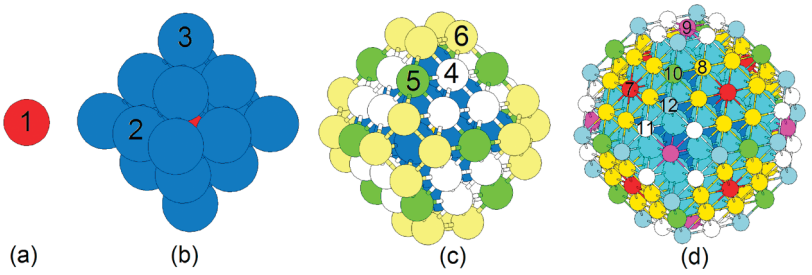

Figure 2. Orbit structure of the odd-numbered truncated octahedra considered in this work: (a) 1-atom TO(1,0); (b) 19-atom TO(3,0), obtained adding 18 atoms to (a); (c) 79-atom TO(5,1), obtained adding 60 atoms to (b); (d) 201-atom TO(7,2), obtained adding 122 atoms to (c). Different symmetry orbits are singled out by different colors and numbers.

dx.doi.org/10.1021/nl200322s |*Nano Lett.* 2011, 11, 1766–1769

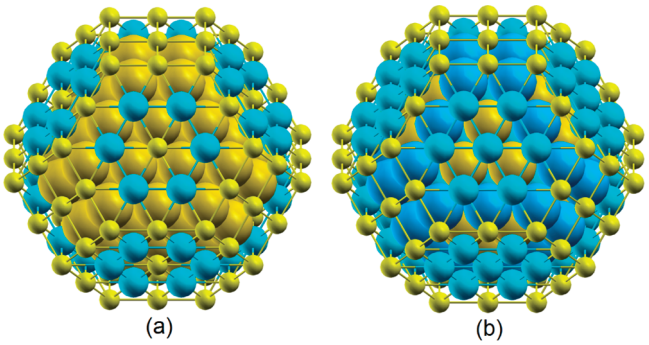

Figure 3. Optimal chemical ordering in a PdPt nanoparticle of size N_{tot} = 201: (a) composition $Pd_{153}Pt_{48}$; (b) composition $Pd_{110}Pt_{91}$ (around 1:1). The view represents atoms of different sizes to highlight the patchy multishell pattern in (b). Atom coloring: yellow for Pd and blue for Pt, with slightly darker shades for the inner shells.

Pd-rich case the 12 Pt atoms preferentially populate the fourth orbit, occupying half of the (111) surface sites, even though the competition with deeper segregation is still strong. In short, doubling the number of Pt atoms changes the segregation sites: there is a close energetic competition between internal and surface or subsurface segregation sites, and this competition is moved in favor of surface with increasing Pt content.

One can wonder whether a different theoretical method may change these results, as it is known that the precise energetics of systems containing third-row transition metals is very sensitive to the details of the theoretical approach.[22] We have thus used an approach involving norm-conserving pseudopotentials and localized basis sets[23] and found that this behavior is fully confirmed (more details in the Supporting Information). Note that in this case the use of symmetry is also beneficial to greatly speed up DFT calculations: we use the NWChem 5.1 quantum chemistry package,[23] which is efficiently parallelized and fully exploits point group symmetry.

116-Atom Particle. The TO(6,2) shown in Figure 1c has also been analyzed, finding results in line with those for the other sizes (more details in the Supporting Information).

201-Atom Particle. The largest (201-atom) nanoparticles here considered exhibit the most outstanding results. This structure corresponds to the TO(7,2) depicted in Figure 2d which is obtained by adding a further shell to the 79-atom TO(5,1). The structure is thus formed by four shells: the inner three are those of the 79-atom cluster, while the fourth one is composed of 116 surface atoms, distinguished into five orbits. As shown in Figure 2d, the (111) facets are regular hexagons.

The results for a single impurity and composition 6-195 show an even more marked tendency of Pt to populate the surface, in agreement with a coordination-dependent bond-energy variations (CBEV) study of 923-atom cuboctahedral PtPt particles.[21] Already a single or few Pt atoms now segregate at the (111) surface, whereas few Pd atoms in a Pt-rich cluster segregate at the corners of the (100) facets. The tendency of Pt to (111)-surface segregation in Pd-rich clusters thus increases with cluster size: at slight variance with CBEV predictions, the (111) surface segregation of a single Pt impurity is only clearly realized when the (111) facets are large enough. Also, with respect to the CBEV, at low Pt contents the center of the facets rather than the near-edge positions is favored (see Table 4 of the Supporting Information). However, similarly to the CBEV results, the tendency of Pt to occupy near-edge sites at (111) is apparent at composition $Pd_{153}Pt_{48}$: the 48 Pt preferentially occupy all the hexagon sites of the (111) surfaces, see Figure 3a, while the structure exhibiting Pt subsurface segregation is higher in energy by 3.82 eV. Thus, the tendency of Pt to (111)-surface segregation is now very strong.

A new picture emerges around composition 1:1. The lowest-energy chemical ordering pattern, e.g., at composition 110-91 is reported in Figure 3b, and it is clearly a multishell arrangement, but of a different kind. As can be drawn from an inspection of this figure, the structure of the fourth shell is such that Pt atoms occupy the center of surface (111) facets, whereas Pd atoms occupy the (100) facets and the edges of the surface shell. However, for the subsurface shell the chemical order is reversed with respect to that of the surface shell: Pd atoms occupy the three central positions of the (111) facets, whereas Pt occupies the (100) facets and the edges. In other words, in correspondence with segregation of Pt at the center of surface facets, we find a segregation of Pd at the center of the underlying facets, and so on. In this segregation pattern, which—to the best of our knowledge—has not been reported before, each shell is a "patchwork" of islands of atoms of the two elements, but the order of the patchwork is reversed in the alternating shells. This is realized in a clear way starting at a sufficiently large size (1.7−1.9 nm) and around composition ≈50−50%. However, this arrangement is not bound to a precise number of atoms but is stable in a *range* of compositions around the equimolar one. As shown in Table 5 of the Supporting Information, we find it favored not only for the nearly equimolar $Pd_{99}Pt_{102}$ and $Pd_{102}Pt_{99}$ particles but also for $Pd_{90}Pt_{111}$ and $Pd_{117}Pt_{84}$. CBEV calculations (which are essentially in tune with DFT results) confirm that this remains true also in the intermediate compositions which are not accessible to our orbit approach, so that we predict it to be stable between at least 45−55% and 58−42% compositions. It can also be recalled in this context that the minimum in the mixing energy (see ref 10 for its definition) for PdPt clusters in this size range at the DFT level is realized at compositions between 30% and 50% in Pt,[20] i.e., in the range in which patchy multishell arrangements are favored.

The origins of this unique chemical ordering can be rationalized in terms of the different behavior of site-energetics of the two elements as a function of the coordination number,[24] i.e., the preferential strengthening of Pt−Pt (and Pt−Pd) intrasurface and Pd−Pd (and Pt−Pd) surface-subsurface bonds, as predicted by the CBEV method.[21] Furthermore, as shown in Table 6 of the Supporting Information in the $Pd_{99}Pt_{102}$ case, the multishell patchy arrangements allow the system to minimize the number of weak Pd−Pd bonds with respect to the stronger Pt−Pt and heterobonds between the two elements, which is energetically advantageous as Pd−Pt mixing is exothermic:[20,30] in a way, the subsurface order is driven by the chemical order of the outer shell.

This peculiar compositional structure can have interesting consequences on the properties of Pd−Pt nanoalloys. Mechanical response[6,7] is expected to be reinforced by a thermodynamically robust and thorough intermixing of the two metals as realized in the patchy arrangement and will be investigated in future work. Catalytic properties of Pd−Pt nanoclusters are likely to be influenced as well.[26] It has been shown in fact that the preference of Pd and Pt clusters toward TO structures is not strongly affected or is even increased[27] in the presence of H adsorption and that Pt−ligand bonding in TO clusters (where Pt lies on a 111 facet) is strengthened by the presence of neighboring Pd atoms.[28] This implies that patchy multishell patterns are

robust to ligand adsorption in realistic conditions, which can even enhance their stability. This may explain the increase in the activity of Pd nanoparticles when Pt is added in the Pd-rich range of compositions.[29]

To conclude, the orbit approach here employed is a powerful tool to explore segregation patterns in nanoscale alloy particles at the first-principles level and will be used in the future also in conjunction with and to further validate effective Hamiltonian methods (e.g., the CBEV approach). The novel type of chemical ordering in nanoalloy clusters (patchy multishell segregation) revealed by first-principle computations is of general interest and is expected to have a significant impact on their properties and on current research in the corresponding area. Indeed, the fact that unusual segregation patterns can occur in nanoparticles even for a pair such as Pd−Pt which presents a nearly ideal solid−solution behavior in the bulk sheds new light on the unexpected possibilities arising at the nanoscale. Experimental verification[1] of the unusual surface segregation of the constituent having larger bulk energy (Pt), and of the corresponding patchy pattern, are desirable.

■ ASSOCIATED CONTENT

Supporting Information. Computational details and tables with a complete set of DFT results. This material is available free of charge via the Internet at http://pubs.acs.org.

■ AUTHOR INFORMATION

Corresponding Author
*E-mail: fortunelli@ipcf.cnr.it.

■ ACKNOWLEDGMENT

A.F. acknowledges financial support from the SEPON project within the ERC-AG programme and from ESF for the workshop on "Computational Nanoalloys" and the MP0903 COST action. DFT calculations were performed at the CINECA Supercomputing Center within the SCONA ISCRA project.

■ REFERENCES

(1) Rousset, J. L.; Renouprez, A. J.; Cadrot, A. M. *Phys. Rev. B* **1998**, *58*, 2150.
(2) Lim, B.; Wang, J.; Camargo, P. H. C.; Jiang, M.; Kim, M. J.; Xia, Y. *NanoLett.* **2008**, *8*, 2535.
(3) Jellinek, J.; Krissinel, E. B. *Chem. Phys. Lett.* **1996**, *258*, 283.
(4) Ferrando, R.; Jellinek, J.; Johnston, R. L. *Chem. Rev.* **2008**, *108*, 845.
(5) Broyer, M.; Cottancin, E.; Lermé, J.; Pellarin, M.; Del Fatti, N.; Vallée, F.; Burgin, J.; Guillon, C.; Langot, P. *Faraday Discuss.* **2008**, *138*, 137.
(6) Chen, H. P.; Kalia, R. K.; Kaxiras, E.; Lu, G.; Nakano, A.; Nomura, K.; van Duin, A. C. T.; Vashishtaa, P.; Yuan, Z. S. *Phys. Rev. Lett.* **2010**, *104*, No. 155502.
(7) Biswas, A.; Siegel, D. J.; Seidman, D. N. *Phys. Rev. Lett.* **2010**, *105*, No. 076102.
(8) Tao, F.; Grass, M. E.; Zhang, Y.; Butcher, D. R.; Renzas, J. R.; Liu, Z.; Chung, J. Y.; Mun, B. S.; Salmeron, M.; Somorjai, G. A. *Science* **2008**, *322*, 932–934.
(9) Paz-Borbón, L. O.; Gupta, A.; Johnston, R. L. *J. Mater. Chem.* **2008**, *18*, 4154.
(10) Fortunelli, A.; Velasco, A. M. *J. Mol. Struct. (THEOCHEM)* **1999**, *487*, 251.
(11) Wales, D., *Energy Landscapes: Applications to Clusters, Biomolecules and Glasses*; Cambridge University Press: Cambridge, 2004.
(12) Giannozzi, P.; et al. *J. Phys.: Condens. Matter* **2009**, *21*, No. 395502.
(13) Vanderbilt, D. *Phys. Rev. B* **1990**, *41*, 7892.
(14) Perdew, J. P.; Burke, K.; Ernzerhof, M. *Phys. Rev. Lett.* **1996**, *77*, 3865.
(15) Baletto, F.; Ferrando, R.; Fortunelli, A.; Montalenti, F.; Mottet, C. *J. Chem. Phys.* **2002**, *116*, 3856.
(16) Paz-Borbòn, L. O.; Mortimer-Jones, T. V.; Johnston, R. L.; Posada-Amarillas, A.; Barcaro, G.; Fortunelli, A. *Phys. Chem. Chem. Phys.* **2007**, *9*, 5202.
(17) Wilson, N. T.; Johnston, R. L. *J. Mater. Chem.* **2002**, *12*, 2913.
(18) Bazin, D.; Guillaume, D.; Pichon, Ch.; Uzio, D.; Lopez, S. *Oil Gas Sci. Technol.* **2005**, *60*, 801.
(19) Cadete-Santos-Aires, F. J.; Geantet, C.; Renouprez, A. J.; Pellarin, M. *J. Catal.* **2001**, *202*, 163.
(20) Fernandez, E. M.; Balbas, L. C.; Perez, L. A.; Michaelian, K.; Garzon, I. L. *Int. J. Mod. Phys. B* **2005**, *19*, 2339.
(21) Rubinovich, L.; Polak, M. *Phys. Rev. B* **2009**, *80*, No. 045404.
(22) Bonačič-Koutecky, V.; Burda, J.; Mitrič, R.; Ge, M.; Zampella, G.; Fantucci, P. *J. Chem. Phys.* **2002**, *117*, 3120.
(23) Bylaska, E. J. et al. *NWChem, A Computational Chemistry Package for Parallel Computers, Version 5.1*; Pacific Northwest National Laboratory: Richland, WA, 2007.
(24) Yang, L.; DePristo, E. *J. Chem. Phys.* **1994**, *100*, 725.
(25) Doye, J. P. K.; Wales, D. J.; Berry, R. S. *J. Chem. Phys.* **1995**, *103*, 4234.
(26) Gonzalez, S.; Neyman, K. M.; Shaikhutdinov, S.; Freund, H.-J.; Illas, F. *J. Phys. Chem. C* **2007**, *111*, 6852.
(27) Calvo, F.; Carre, A. *Nanotechnology* **2006**, *17*, 1292.
(28) West, P. S.; Johnston, Roy L.; Barcaro, G.; Fortunelli, A. *J. Phys. Chem. C* **2010**, *114*, 19678.
(29) Toshima, N.; Yonezawa, T. *New J. Chem.* **1998**, *1179*, 1179.
(30) Paz-Borbon, L. O.; Johnston, R. L.; Barcaro, G.; Fortunelli, A. *J. Phys. Chem. C* **2007**, *111*, 2936.

■ NOTE ADDED AFTER ASAP PUBLICATION

The TOC and abstract artwork was modified in the version of this paper published March 2, 2011. The correct version published March 8, 2011.